公益財団法人矢崎科学技術振興記念財団
国際交流援助　研究発表　帰国報告書

公益財団法人矢崎科学技術振興記念財団
　理事長 殿

国際学術会議での研究発表を終えて帰国しましたので、下記の通り報告します。

2025 年　10 月　15 日
氏名　野島 渉平
所属　東北大学 金属材料研究所 強磁場超伝導材料研究センター
職位　博士後期課程 2 年

1. 発表論文名
A numerical study on the impact of edge impregnation: Screening current-induced strain/stress in REBCO insert for 33T-CSM
33T-CSM 用内挿 REBCO コイルにおける遮蔽電流誘起応力・ひずみ数値解析：端面含浸の効果

2. 国際学術会議の名称
17th European Conference on Applied Superconductivity (EUCAS2025)
ヨーロッパ応用超電導学会 2025

4. 国際学術会議の開催地（国、地名、会場名など）
ポルトガル（ポルト），Porto Alfandega Congress Center

5. 渡航期間
2025 年 9 月 20 日 ～ 2025 年 9 月 28 日

6. 国際学術会議発表の要旨
　私たちは，世界最高クラスの強磁場を生み出せる「超伝導マグネット」の研究を進めている．超伝導とは，ある温度以下で電気抵抗がゼロになる現象であり，この性質をもつ超伝導線を巻いて作られたコイルを「超伝導コイル」と呼ぶ．従来の銅線コイルでは流せる電流に限界があり，電気抵抗によるエネルギーロスも大きいため，強磁場の発生が難しいという課題があった．一方，超伝導マグネットは極低温での冷却を必要とするが，大電流をほぼ損失なく流すことができるため，従来技術では得られなかった高磁場を効率的に発生させることが可能である．
　このような超伝導マグネットが生み出す強磁場は，医療・分析機器や交通・エネルギー・基礎科学など，多様な分野で活用されている．医療・分析分野では MRI（磁気共鳴画像装置）や NMR（核磁気共鳴）装置に用いられ，交通分野ではリニアモーターカーの浮上や推進に応用されている．また，核融合炉の磁場閉じ込め装置や高エネルギー加速器などの大型科学装置にも不可欠であり，さらに，高磁場環境を利用することで，新しい量子現象の観測や物質科学の発展にも寄与している．
　私たちは現在，定常磁場として世界最高となる 33 テスラ無冷媒超伝導マグネットの開発に取り組んでいる．しかし，このような高磁場マグネット内部では非常に強い電磁力（ローレンツ力）が発生し，コイルの変形や損傷を引き起こすおそれがある．そのため，「強い磁場を安全かつ安定に発生させるための構造設計」が重要な研究課題となっている．
　今回の発表では，「遮蔽電流誘起応力・ひずみ（SCIS）」と「端面含浸超伝導コイル」という 2 つのテーマを扱った．SCIS とは，超伝導コイル内部に生じる遮蔽電流がコイルに余分な力を加える現象であり，これがコイルの変形や破損を引き起こし，高磁場マグネットの性能を制限する要因

となる．一方，「端面含浸」はコイルを補強するための新しい構造である．「含浸」とは樹脂でコイルを固めることを指すが，従来のように全体を含侵すると，冷却時の熱応力によって超伝導線が劣化する問題がある．そこで私たちは，コイルの端部のみを部分的に補強する「端面含浸」という方法を考案し，この手法によって超伝導線を劣化させることなくコイルを強化できることを実験的に確認した．

しかし，端面含浸構造が SCIS にどのような影響を受けるかは明らかでなかった．そこで数値解析を行った結果，SCIS が端面含浸コイルに大きな変形を引き起こすことを発見した．さらに，SCIS を低減する新たな方法として，コイル内部の一部を意図的に接着させる構造を提案し，これにより SCIS によって生じる余分な力をほぼ完全に打ち消せることを見いだした．学会発表では，これらの解析結果と低減手法を報告し，「非常に独創的で有効な発想だ」と高い評価を得た．特に，SCIS 低減効果の大きさが注目を集めた．

今回の発表を通じて，私たちの研究が国際的にも関心を集めていることを実感した．今後は，より大規模なマグネットでの実証実験を進め，世界最高磁場の実現に向けて研究をさらに発展させていく予定である．

7．国大学術会議の動向

今回の国大学術会議では，超伝導研究の幅広い分野から最新の成果が報告された．発表内容は大きく分けて，「高磁場マグネットの開発」，「超伝導線の開発・評価」，「超伝導の量子効果を利用した応用」の 3 つの分野に整理される．

まず，高磁場マグネット開発の分野では，超高磁場超伝導マグネット，核融合炉用超伝導マグネット，および航空機用回転機などの交流応用向けマグネット技術に関する報告が多く見られた．超高磁場マグネットに関しては，アメリカ，中国，ヨーロッパ，日本（私たち）からそれぞれ研究成果が発表されており，世界的な技術競争の激化がうかがえた．核融合炉用マグネットの分野では，ヨーロッパの核融合スタートアップ企業 Proxima Fusion が，次世代核融合炉に向けた超伝導マグネット開発の進捗を報告し，大きな注目を集めていた．また，航空機や産業用モータなどに応用される交流用超伝導マグネットの研究報告も増加しており，超伝導技術がより実用的な分野へと拡大していることが印象的であった．

次に，超伝導線の開発・評価分野では，より高い臨界電流密度を達成しつつ，高品質な超伝導線材を製造するための研究が活発に行われていた．大学や研究機関のみならず，超伝導線メーカーからの発表も多く，基礎研究から実用化に向けた開発体制が整いつつあることが示された．特に，REBCO 線材の高性能化や長尺化を目指した取り組みが注目を集めていた．

さらに，超伝導の量子効果を応用した研究分野では，量子コンピュータや量子センサーに関連する報告が多数あった．学術的にも産業的にも重要な課題が議論されており，この分野の活発な発展が感じられた．

全体として，本会議では「高磁場化」「高性能化」「量子応用」という 3 つの潮流が，今後の超伝導研究の主要な方向性として明確に示された．基礎から応用まで多角的な研究が展開されており，超伝導技術が今後さらに多様な分野へ波及していくことが期待される．

以上

Screening Current-Induced Stress in Edge-Impregnated REBCO Coils for 33T-CSM

Shohei Nojima, Yuji Tsuchiya, Alexandre Zampa, Arnaud Badel, Yoh Nagasaki, Makoto Tsuda and Satoshi Awaji

***Abstract*—Edge impregnation is a key technology for fabricating robust, high-field REBCO insert magnets. However, the effect of screening current-induced stress (SCIS), a critical challenge in ultra-high field magnet design, has not been fully clarified. This study aims to investigate the influence of SCIS on edge-impregnated REBCO coils through an electromagnetic-mechanical analysis. The investigation focuses on the 33 T cryogen-free superconducting magnet (33T-CSM) under development at HFLSM, Tohoku University. The analysis revealed that SCIS significantly amplified the hoop strain in edge-impregnated coils, predicting a maximum strain exceeding the conductor's irreversible limit. Compared with the full impregnation, the edge impregnation was insufficient to suppress SCIS to the acceptable level even with mechanical reinforcement although it made the delamination stress negligible. Notably, the analysis overestimated the hoop strain compared with experiments because the large-scale prototype coil (33T-LPC) has been successfully validated without degradation. Possible origins for the overestimation are discussed, including interfacial friction between the stacked pancake coils.**

***Index Terms*—Edge impregnation, REBCO coil, screening current induced stress (SCIS), ultra-high field superconducting magnet.**

I. INTRODUCTION

In recent years, the development of ultra-high field superconducting magnets has been actively pursued worldwide. This progress includes the successful operation of several key magnets, such as the 32 T all-superconducting magnet at the National High Magnetic Field Laboratory (NHMFL) [1], the 32.35 T magnet at the Institute of Electrical Engineering, Chinese Academy of Sciences (IEE CAS) [2], the 25 T cryogen-free superconducting magnet at the High Field Laboratory for Superconducting Materials (HFLSM) [3], and the Little Big Coil exceeding 45 T at NHMFL [4]. Many of these achievements rely on REBCO conductors, which have demonstrated high potential in terms of both critical current and mechanical strength [1], [2], [4], [5]. Building on these successes, even more ambitious projects are now underway, such as a 40 T superconducting magnet at NHMFL [6], a 35 T magnet at IEE CAS [7], a 40 T magnet at CEA [8], NMR magnets exceeding 30 T at RIKEN , MIT, and Bruker [9], [10], [11] and a 40 T magnet for a muon collider at CERN [12]. In line with this global trend, a 33 T cryogen-free superconducting magnet (33T-CSM) is currently under development at HFLSM, Tohoku University [13]. The 33T-CSM is composed of a 14 T LTS outsert magnet and a 19 T REBCO insert magnet. The REBCO insert employs a "robust structure" that incorporates several key features [14]:

(1) all turn separated by co-wound fluorine-coated polyimide tape,
(2) face-to-back 2-tape bundled REBCO conductor,
(3) REBCO tape with a 40 μm-thick copper stabilizer layer,
(4) edge impregnation combined with FRP plates.

Edge impregnation has been shown to effectively reduce the maximum hoop stress/strain under uniform current conditions [15], [16]. In fact, a large-scale prototype coil for the 33T-CSM (33T-LPC), consisting of 20 stacked REBCO pancake coils with the robust structure, successfully generated a magnetic field of 25 T under 14 T background field [16], [17].

However, a significant challenge in the development of ultra-high field magnets is the electromagnetic stress/strain induced by screening currents (SCIS) [18], [19], [20], [21], [22], [23]. Previous studies have reported that SCIS can cause large localized tensile and compressive stresses, potentially leading to plastic deformation or buckling of the REBCO tape [1], [17], [21]. While fully impregnated REBCO coils have been reported to mitigate SCIS, they remain susceptible to delamination stress [20], [24], [25]. In contrast, the influence of SCIS on edge-impregnated REBCO coils has not yet been clarified [15], [16], [26].

Therefore, this study investigates the influence of SCIS on edge-impregnated REBCO coils using numerical analysis. The primary design target is to maintain the strain in the REBCO conductor below its irreversible limit of 0.4% [27], [28]. Our approach is to investigate the fundamental impact of SCIS, compare the mechanical stiffness of coils with different impregnation methods, and validate the numerical models against available experimental data.

Manuscript received -- ---- 20--; revised -- ---- 20--, accepted -- ---- 20--. Date of publication -- ---- 20--; date of current version -- ---- 20--. This work was supported in part by Moonshot R&D - MILLENNIA Program Grant Number JPMJMS24A2. *(Corresponding author: Satoshi Awaji).*

Shohei Nojima, Yuji Tsuchiya, and Satoshi Awaji are with the Institute for Materials Research, Tohoku University, Sendai 980-8577, Japan (e-mail: satoshi.awaji.e8@tohoku.ac.jp).

Alexandre Zampa is with the Institute for Solid State Physics, University of Tokyo, Kashiwa, Chiba 277-8581, Japan.

Arnaud Badel is with the G2Elab/Néel Institute, CNRS, University of Grenoble Alpes, 38042 Grenoble, France.

Shohei Nojima, Yoh Nagasaki, Makoto Tsuda are with the Department of Electrical Engineering, Graduate School, Tohoku University, Sendai 980-8579, Japan

Color versions of one or more of the figures in this article are available online at http://ieeexplore.ieee.org

II. Numerical Analysis Method

A. Analysis target

A sequential electromagnetic-mechanical analysis was performed using COMSOL Multiphysics for the 2 magnets [19], [24], [25], [29]: 33T-CSM and 33T-LPC. The two magnets differ mainly in the number of stacked pancake coils and the use of reinforcement tape.

The investigation began with a focus on the 33T-CSM. First, to investigate the fundamental impact of SCIS on an edge-impregnated REBCO coil, the hoop strain was compared between cases with and without screening currents. Second, to assess the effect of the impregnation method on SCIS, the hoop strain and radial stress were compared among three distinct coil types: edge impregnation, dry winding, and full impregnation. Finally, the focus shifted to the 33T-LPC, for which the hoop strain was calculated numerically and compared with available experimental data.

B. Analysis method

Table 1 shows the specifications of the magnets [13], [17]. In the electromagnetic model, the screening current distribution was computed using the homogenized T-A method [30], [31], and the magnetic field dependence of the critical current, $I_c(B)$ was shown in Figure 1 and described by a modified Kim model [32], [33], [34] fitted to in-house experimental data up to 24 T [35], [36], [37], [38],

$$I_c(B) = I_c(B_r) = \frac{I_c(0)}{(1 + |B_r|/B_0)^{\alpha}} \quad (1)$$

where B_r is radial magnetic field component, B_0 and α are the fitting parameter assuming the REBCO tapes with $I_c = 220$ A at 77.3 K self-field, which are shown in Fig. 1. Current-voltage characteristics were formulated by the n-value model where n was fixed as 20.

In the structural analysis, the Lorentz force density ($J \times B$), obtained from the electromagnetic analysis, was applied to the domains representing the REBCO tapes. All materials were assumed to be linear elastic with isotropic Young's moduli. For the contact condition, a penalty method was used between tapes in the edge-impregnated and dry-wound coils where no epoxy was present, while a bonded condition was applied to the fully impregnated coil. The bottom surface of the coil was fixed in the z-direction by applying a displacement boundary condition of $u_z = 0$.

TABLE I
SPECIFICATIONS OF THE ANALYSIS FOR 33T-CSM & 33T-LPC

Parameters	Unit	33T-CSM	33T-LPC
Magnet design			
Total center field	T	33	25
Center field of LTS magnet	T	14	14
Center field of REBCO magnet	T	19	11
REBCO magnet [13], [17]			
# of pancakes	-	64	20
# of turns per pancake	-	246	279
# of strands of REBCO tape	-	2	
Size of REBCO tape	mm	$4.1^{\text{width}} \times 0.15^{\text{thick}}$	
Thickness of reinforcement tape	mm	Hastelloy, 0.1	-
Thickness of insulation tape	mm	Fluorine-coated polyimide, 0.055	
Inner radius, R_{in}	mm	34	
Outer radius, R_{out}	mm	147.2	133
Height	mm	324.5	101
Thickness of edge epoxy	mm	0.220	
Thickness of FRP plate	mm	0.180	
Operation current	A	361	300
Operation temperature	K	10	4.2
REBCO tape			
Manufacturer	-	Fujikura	
Product name	-	FESC-SCH04(40)	
Thickness of substrate	mm	0.05	
Thickness of Cu stabilizer	mm	0.04/side	
Critical current, $I_c(0)$	A	3016	2685
Fitting parameter, B_0	T	2.95	2.81
Fitting parameter, α	-	1.04	0.93
Young's moduli			
REBCO tape	GPa	125	
Reinforcement tape	GPa	205	-
Insulation tape	GPa	3.4	
Edge epoxy	GPa	18	
FRP plate	GPa	30	

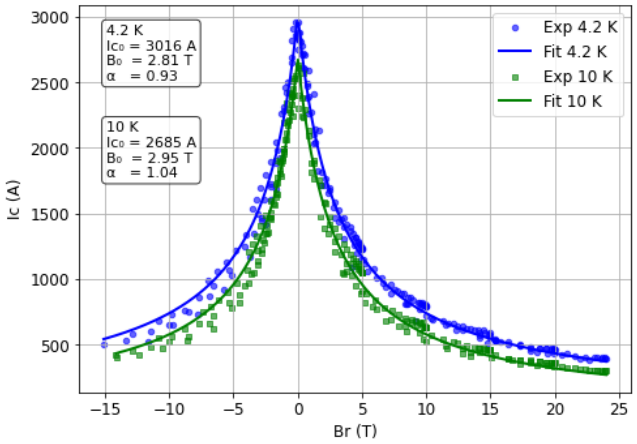

Fig. 1. Magnetic field dependence of the critical current of the REBCO tapes with fitting curves using the modified Kim model.

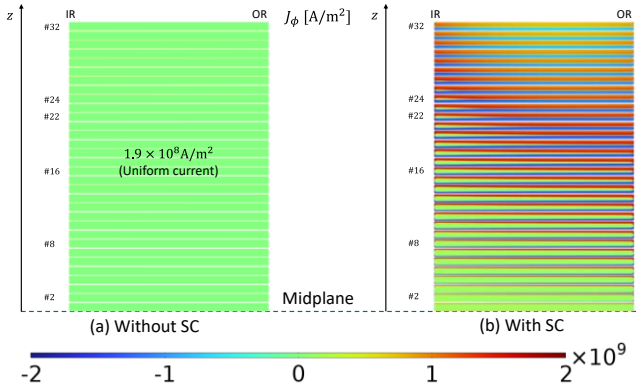

Fig. 2. Current density (a) without and (b) with screening current at 361 A/33 T in 33T-CSM. Only half of the magnet is modeled using symmetry.

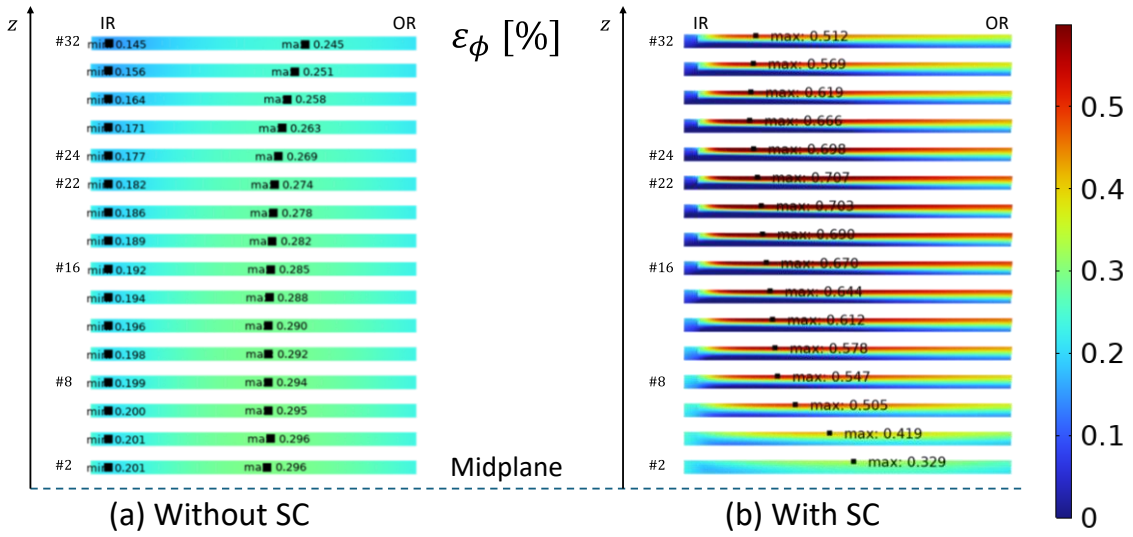

Fig. 3. Hoop strain distribution in 33T-CSM (a) without and (b) with screening current. Only even-numbered pancakes are shown. Square dots indicate the maximum strain in the pancakes.

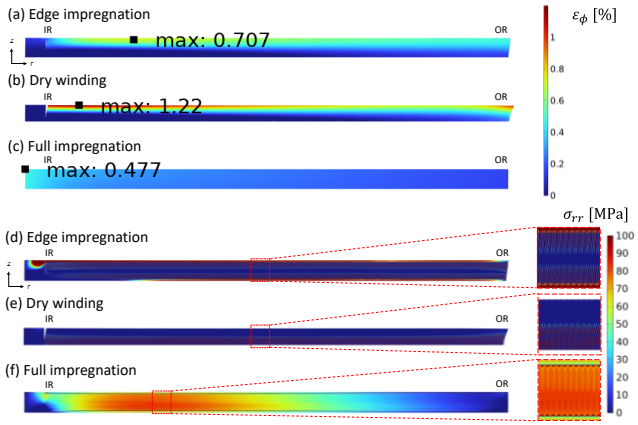

Fig. 4. (a-c) Hoop strain and (d-f) radial stress distributions in the #22 pancake for edge-impregnated, dry-wound, and fully-impregnated coils, considering screening current.

III. Analysis Results and Discussions

A. SCIS in edge-impregnated REBCO coil of 33T-CSM

Figure 2 shows the current density distribution under two conditions: (a) assuming a uniform transport current and (b) incorporating the screening current. While the former case exhibits a homogeneous current flow, the latter shows a highly non-uniform distribution, characterized by large, localized current densities induced at the tape edges. The screening current penetrates more deeply from the middle to the top pancakes. As the radial magnetic field (B_r) increases for the larger # of the pancakes, the screening current extends over the entire tape width around at pancake #, resulting in a decrease of I_c at the top pancake.

Figure 3 shows the hoop strain distributions (a) without and (b) with screening current. Without screening current, the maximum hoop strain was approximately 0.3% in the central

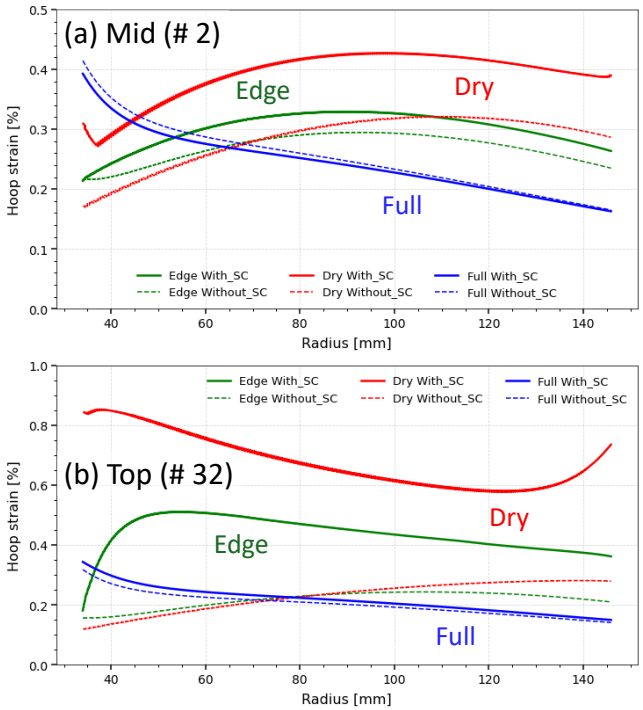

Fig. 5. Hoop strain on the upper edge of the REBCO tapes (solid) with and (dashed) without screening current for (a) the mid-pancake coil #2 and (b) the top pancake coil #32.

pancake coil, which is consistent with our previous study [15], [16] and remains below the strain limit of 0.4%. In contrast, as shown in Fig. 3 (b), the maximum hoop strain reached approximately 0.7% at the #22 pancake coil, that significantly exceeds the allowable design criterion. The reason why the hoop strain reaches its maximum at about 70% of the coil height from the middle plane is considered to be the balance between the decrease in I_c due to the increase in B_r and the expansion of the screening current region.

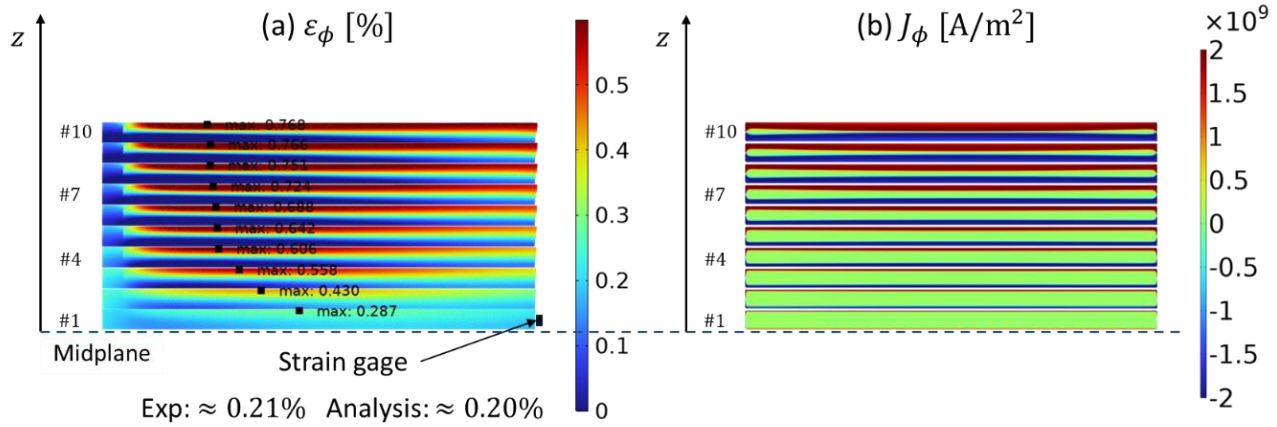

Fig. 6. Analytical results for the 33T-LPC at 300 A / 25 T, showing (a) hoop strain and (b) current density distributions. The hoop strain at the outermost turn of the mid-pancake is compared with experimental data.

B. Comparison of the impregnation methods in 33T-CSM

To compare the impregnation technique, the analysis focused on the #22 pancake coil, as this was where $\varepsilon_{\phi\_\max}$ was observed when considering SCIS (as shown in Fig. 3). Figure 4 presents the (a-c) hoop strain and (d-f) radial stress distributions in the #22 REBCO pancake coil for the edge-impregnated, dry-wound, and fully-impregnated coils, with the effects of screening currents included. An analysis of the hoop strain (Fig. 4(b)) reveals that while the dry-wound coil exhibits a substantial maximum strain ($\varepsilon_{\phi\_\max} \approx 1.2\%$), the fully-impregnated coil effectively suppresses SCIS, with its maximum strain remaining at the design limit ($\varepsilon_\phi \approx 0.4\%$). These trends are consistent with those reported in previous studies [17], [18], [19], [21], [24], [25]. Meanwhile, with respect to the radial stress (Fig. 4(d, e)), the REBCO tapes in both the edge-impregnated and dry-wound coils experience no delamination stress. This is attributed to the absence of epoxy between the tapes, which prevents the propagation of radial tensile stress. In contrast, the fully impregnated coil experiences a significant delamination stress ($\sigma_{rr} \approx 80$ MPa), which poses a potential risk of degradation ($\sigma_{rr} > 10$MPa) [34]. Therefore, it is found that while edge impregnation prevents delamination stress, the reinforcement it provides is insufficient to fully suppress the large strain induced by SCIS.

Figure 5 shows the hoop strain along the radial direction on the upper edge of the REBCO tape for (a) a mid-pancake coil #2 and (b) a top pancake coil #32. The dashed and solid lines represent the results without and with screening currents, respectively. Without screening currents, the edge impregnation reduces the maximum hoop strain in both the mid and top pancakes, a trend consistent with previous research [15], [16]. For the mid-pancake coil, where the influence of the screening current is minimal, a similar result is obtained even when SCIS is considered. However, in the top pancake coil, which is strongly affected by screening currents, the hoop strain increased from 0.3% to 0.8% in the dry coil and from 0.25% to 0.51% in the edge-impregnated coil, highlighting the large impact of the screening current.

C. Comparison of analysis and experiment for the 33T-LPC

The preceding analysis predicted that SCIS would exert a significant influence on edge-impregnated coils. To validate this, the calculated SCIS in the 33T-LPC was compared with available experimental data from its successful test to 25 T in a 14 T background field [17]. Figure 6 shows the analytical results for (a) hoop strain and (b) current density distributions. The analysis shows good agreement with the experiment for the central pancake coil #1, where a strain of 0.20% was calculated, consistent with the 0.21% measured by a strain gauge on the outermost turn. For the other pancake coils, however, the analysis predicts that the hoop strain exceeds the 0.4% limit in all cases, reaching a maximum of 0.77%. Since the magnet operated without any degradation, this indicates that our model is likely to overestimate the strain in the pancake coils other than the mid-pancake.

D. Discussion

Here, we discuss the potential reasons for this significant overestimation of strain. First, as reported in previous studies, the overestimation could be partially resolved by incorporating factors neglected in our analysis, such as winding stress, thermal strain from cooldown, and the tilting effect of the REBCO tapes [24], [25], [29], [31], [34], [40].

In addition to these factors, we believe the overestimation is primarily resolved by the interfacial friction between coils in the magnet's stacked structure. The 33T-LPC consists of 20 stacked pancake coils subjected to a large axial compressive force from both initial pre-compression and electromagnetic attraction during operation. This compressive force generates friction at the contact surfaces between the coils, providing a mechanical constraint against hoop strain and suppressing SCIS because of the opposing stress/strain between adjoining pancake surfaces. Hence, gluing the adjoining pancakes may be effective to reduce SCIS. This mechanism could explain the successful operation despite the high predicted strain, and its effects will be examined in future work.

IV. Conclusion

The effect of screening current-induced stress (SCIS) on edge-impregnated REBCO coils was investigated through numerical analysis. The findings of this work are as follows:

1) The analysis revealed that SCIS causes the hoop strain to reach 0.7% in the 19 T REBCO insert magnet, which significantly exceeds the conductor's irreversible strain limit of 0.4%. While edge impregnation successfully avoids the delamination stress seen in fully impregnated coils, its mechanical reinforcement alone is insufficient to suppress the large strain induced by screening current.
2) The analysis may significantly overestimate the hoop strain when compared with experimental observations. While the numerical model predicted the prototype coil would experience strains over the degradation limit, the magnet was successfully operated without any damage. This suggests that additional contributions such as the friction between adjoining pancakes to suppress the strain should be considered.

In conclusion, our analysis shows that SCIS significantly affects edge-impregnated REBCO coils, but it overestimates the strain in the actual magnet. This overestimation is likely due to interfacial friction between pancake coils, which will be investigated in future work.

Acknowledgment

The authors would like to thank K. Takahashi at HFLSM, T. Okada at Kyushu Institute of Technology, and T. Uto, H. Takewa, S. Hanai, S. Ioka, and J. Inagaki at Toshiba Energy System & Solutions Corporation for providing valuable information and material property data for the large-scale prototype coil of 33T-CSM. We also thank T. Yamaguchi and Y. Takahashi at Keisoku Engineering System, and T. Kinoshita and T. Hasebe at Foundation for Computational Science for valuable discussions on numerical analysis. We are also grateful to Y. Suetomi at NHMFL for helpful advice on the numerical analysis.

References

[1] H. W. Weijers *et al.*, "Progress in the development and construction of a 32-T superconducting magnet," *IEEE Trans. Appl. Supercond.*, vol. 26, no. 4, pp. 1–7, June 2016.
[2] J. Liu *et al.*, "World record 32.35 tesla direct-current magnetic field generated with an all-superconducting magnet," *Supercond. Sci. Technol.*, vol. 33, no. 3, p. 03LT01, Mar. 2020.
[3] S. Awaji *et al.*, "First performance test of a 25 T cryogen-free superconducting magnet," *Supercond. Sci. Technol.*, vol. 30, no. 6, p. 065001, June 2017.
[4] S. Hahn *et al.*, "45.5-tesla direct-current magnetic field generated with a high-temperature superconducting magnet," *Nature*, vol. 570, no. 7762, pp. 496–499, June 2019.
[5] C. Yao and Y. Ma, "Superconducting materials: Challenges and opportunities for large-scale applications," iScience, vol. 24, no. 6, p. 102541, June 2021.
[6] H. Bai *et al.*, "The 40 T superconducting magnet project at the national high magnetic field laboratory," *IEEE Trans. Appl. Supercond.*, vol. 30, no. 4, pp. 1–5, June 2020.
[7] X. Zhang *et al.*, "Strain analysis and preliminary test of an all-superconducting high-field magnet generating 32.4 T direct-current magnetic field," *Supercond. Sci. Technol.*, vol. 37, no. 12, p. 125003, Dec. 2024.
[8] T. De Chabannes *et al.*, "Mechanical conception and calculation of HTS insert for the 40+ T all superconducting magnet of the FASUM project," EUCAS 2025, 1-LP-HF1-56, Porto, Portugal, 2025.
[9] K. Naito *et al.*, "Analyses of deformation due to screening-current-induced force in layer-wound REBCO insert coil for 1.3-GHz LTS/HTS NMR," *IEEE Trans. Appl. Supercond.*, vol. 33, no. 5, pp. 1–5, Aug. 2023.
[10] D. Park *et al*, "Design overview of the MIT 1.3-GHz LTS/HTS NMR magnet with a new REBCO insert," *IEEE Trans. Appl. Supercond.*, vol. 31, no. 5, pp. 1–6, Aug. 2021.
[11] P. Wikus *et al*, "Commercial gigahertz-class NMR magnets," *Supercond. Sci. Technol.*, vol. 35, no. 3, p. 033001, Mar. 2022.
[12] S. Fabbri *et al.*, "Magnets for a Muon Collider," *J. Phys. Conf. Ser.*, vol. 2687, no. 8, p. 082016, Jan. 2024.
[13] S. Awaji *et al.*, "Progress of 33 T cryogen-free superconducting magnet project at HFLSM," *IEEE Trans. Appl. Supercond.*, vol. 35, pp. 1–6, 2025.
[14] S. Awaji *et al.*, "Robust REBCO insert coil for upgrade of 25 T cryogen-free superconducting magnet," *IEEE Trans. Appl. Supercond.*, vol. 31, no. 5, pp. 1–5, Aug. 2021.
[15] A. Badel *et al.*, "Conceptual design of a 33 T cryogen-free magnet REBCO insert: Mechanical aspects and protection against thermal runaway," *IEEE Trans. Appl. Supercond.*, vol. 34, no. 5, pp. 1–5, Aug. 2024.
[16] A. Badel *et al.*, "First validation of robust REBCO insert concept on a large 20-pancake prototype reaching up to 25 T," *IEEE Trans. Appl. Supercond.*, vol. 33, no. 5, pp. 1–5, Aug. 2023.
[17] K. Takahashi *et al.*, "Performance test of 20-stacked two-tapes-bundled REBCO pancake coils for upgrading of 25-T cryogen-free superconducting magnet to 30 T," *IEEE Trans. Appl. Supercond.*, vol. 33, no. 5, pp. 1–5, Aug. 2023.
[18] P. C. Michael *et al.*, "Assembly and test of a 3-nested-coil 800-MHz REBCO insert (H800) for the MIT 1.3 GHz LTS/HTS NMR magnet," *IEEE Trans. Appl. Supercond.*, vol. 29, no. 5, pp. 1–6, Aug. 2019.
[19] J. Xia *et al*, "Stress and strain analysis of a REBCO high field coil based on the distribution of shielding current," *Supercond. Sci. Technol.*, vol. 32, no. 9, p. 095005, Sept. 2019.
[20] S. Takahashi *et al.*, "Hoop stress modification, stress hysteresis and degradation of a REBCO coil due to the screening current under external magnetic field cycling," *IEEE Trans. Appl. Supercond.*, vol. 30, no. 4, pp. 1–7, June 2020.
[21] X. Hu *et al.*, "Analyses of the plastic deformation of coated conductors deconstructed from ultra-high field test coils," *Supercond. Sci. Technol.*, vol. 33, no. 9, p. 095012, Sept. 2020.
[22] Y. Yan, Y. Li, and T. Qu, "Screening current induced magnetic field and stress in ultra-high-field magnets using REBCO coated conductors," *Supercond. Sci. Technol.*, vol. 35, no. 1, p. 014003, Jan. 2022.
[23] Y.-H. Zhou, D. Park, and Y. Iwasa, "Review of progress and challenges of key mechanical issues in high-field superconducting magnets," *Natl. Sci. Rev.*, vol. 10, no. 3, p. nwad001, Mar. 2023.
[24] H. Ueda *et al*, "Numerical evaluation of the deformation of REBCO pancake coil, considering winding tension, thermal stress, and screening-current-induced stress," *Supercond. Sci. Technol.*, vol. 34, no. 2, p. 024003, Feb. 2021.
[25] H. Ueda *et al*, "Experiment and numerical simulation of the combined effect of winding, cool-down, and screening current induced stresses in REBCO coils," *Supercond. Sci. Technol.*, vol. 35, no. 5, p. 054001, May 2022.
[26] T. Uto *et al.*, "Basic design of REBCO insert coil of 33 T cryogen-free superconducting magnet," *IEEE Trans. Appl. Supercond.*, vol. 35, no. 5, pp. 1–5, 2025.
[27] Fujikura Ltd., "Introduction to rare-earth HTS tapes," Internal report, Rev. JUL2024, Jul. 2024. [Online]. Available: https://www.fujikura.co.jp/products/superconductors/images/Fujikura_superconductor_202407_JP.pdf. Accessed: Oct. 10, 2025.
[28] S. Kume *et al.*, " Large-current Electro-Mechanical Characteristic of REBCO Tapes over a Wide Temperature Range Using Pulsed Current," to be submitted to *IEEE Trans. Appl. Supercond.*, 2025.
[29] M. Niu *et al*, "Numerical analysis of the electromechanical behavior of high-field REBCO coils in all-superconducting magnets," *Supercond. Sci. Technol.*, vol. 34, no. 11, p. 115005, Nov. 2021.
[30] E. Berrospe-Juarez *et al*, "Real-time simulation of large-scale HTS systems: multi-scale and homogeneous models using the T–A formulation," *Supercond. Sci. Technol.*, vol. 32, no. 6, p. 065003, June 2019.

[31]D. Kolb-Bond *et al*, “Screening current induced field changes during DE-energization with axial clamping,” *IEEE Trans. Appl. Supercond.*, vol. 32, no. 6, pp. 1–4, Sept. 2022.

[32]Y. B. Kim, C. F. Hempstead, and A. R. Strnad, “Magnetization and Critical Supercurrents,” *Phys. Rev.*, vol. 129, no. 2, pp. 528–535, Jan. 1963.

[33]E. Pardo *et al*, “Low-magnetic-field dependence and anisotropy of the critical current density in coated conductors,” *Supercond. Sci. Technol.*, vol. 24, no. 6, p. 065007, June 2011.

[34]Y. Yan *et al.*, “Screening-current-induced mechanical strains in REBCO insert coils,” *Supercond. Sci. Technol.*, vol. 34, no. 8, p. 085012, Aug. 2021.

[35]Y. Tsuchiya *et al.*, “Flux pinning landscape up to 25 T in SmBa2Cu3Oyfilms with BaHfO3nanorods fabricated by low-temperature growth technique,” *Supercond. Sci. Technol.*, vol. 30, no. 10, p. 104004, Oct. 2017.

[36]Y. Tsuchiya *et al*, “Critical current measurements of HTS tapes using pulsed current in high fields at low temperatures,” *IEEE Trans. Appl. Supercond.*, vol. 33, no. 5, pp. 1–5, Aug. 2023.

[37]Y. Tsuchiya *et al*, “Characterization of in-field critical currents in REBCO tapes over wide temperature range by pulsed current source with supercapacitor,” *IEEE Trans. Appl. Supercond.*, vol. 34, no. 5, pp. 1–7, 2024.

[38]Y. Tsuchiya *et al*, “Critical current evaluation of REBCO tapes across entire temperatures and magnetic fields up to 25 T using a 5 kA pulsed current supply,” *IEEE Trans. Appl. Supercond.*, vol. 35, pp. 1–5, 2025.

[39]H. Maeda and Y. Yanagisawa, “Recent developments in high-temperature superconducting magnet technology (review),” *IEEE Trans. Appl. Supercond.*, vol. 24, no. 3, pp. 1–12, June 2014.

[40]Y. Suetomi *et al.*, “Screening current induced stress/strain analysis of high field REBCO coils with co-winding or over-banding reinforcement,” *IEEE Trans. Appl. Supercond.*, vol. 34, no. 5, pp. 1–6, Aug. 2024.